POLİTEKNİK DERGİSİ

JOURNAL of POLYTECHNIC

ISSN: 1302-0900 (PRINT), ISSN: 2147-9429 (ONLINE)
URL: http://dergipark.gov.tr/politeknik

A numerical investigation on oblique projectile impact behavior of AA5083-H116 plates

AA5083-H116 levhaların açılı mermi çarpma davranışı üzerine sayısal bir araştırma

***Yazar(lar) (Author(s))**: Selim GÜRGEN*

ORCID: 0000-0002-3096-0366

Bu makaleye şu şekilde atıfta bulunabilirsiniz(To cite to this article): Gürgen S., "A numerical investigation on oblique projectile impact behavior of AA5083-H116 plates", ***Politeknik Dergisi***, 22(2): 293-301, (2019).

Erişim linki (To link to this article): http://dergipark.gov.tr/politeknik/archive

DOI: **10.2339/politeknik.403994**

A Numerical Investigation on Oblique Projectile Impact Behavior of AA5083-H116 Plates

Araştırma Makalesi / Research Article

Selim GÜRGEN*

Eskişehir Vocational School, ESOGU, 26110, Eskişehir, Turkey

(Geliş/Received : 14.01.2018 ; Kabul/Accepted : 06.02.2018)

ABSTRACT

In this paper, oblique impact of ogive nose projectile on 5083-H116 aluminum alloy plates was numerically investigated. Three parameters such as impact velocity, impact angle and target configuration were varied to observe their influence on the ballistic resistance of targets. Based on the results, the oblique angle of impact acts an important role on the deformation mode of targets. The penetration of projectile dominates targets under low oblique angle impacts and the deformation changes from embedment to ricochet as oblique angle increases. Beside the oblique angle, the ballistic resistance of target is heavily dependent on impact velocity. Targets are perforated as impact velocity increases even if oblique angle becomes larger. Target configuration is another factor on the protective performance which is increased using thicker plates. The ballistic response of monolithic and double layer targets for the same thickness is very close each other.

Keywords: Armor plate, aluminum, ballistic impact, finite element method.

AA5083-H116 Levhaların Açılı Mermi Çarpma Davranışı Üzerine Sayısal Bir Araştırma

ÖZ

Bu çalışmada sivri uçlu mermilerin AA5083-H116 levha üzerine açılı çarpma durumları sayısal olarak incelenmiştir. Çalışmada çarpma hızı, çarpma açısı ve hedef konfigürasyonu değişken olarak tutularak bu değişkenlerin hedef balistik direncine olan etkileri araştırılmıştır. Sonuçlara göre, çarpma açısının hedef hasarı üzerinde önemli rol oynadığı belirlenmiştir. Düşük eğimli çarpmalarda hedef delinmesinin baskın olduğu ancak eğim açısındaki artışın mermi gömülmesine ve merminin sekmesine sebep olduğu gözlenmiştir. Mermi hızının yüksek olduğu durumlarda ise eğim açısı fazla olsa bile hedefte delinme gerçekleşmektedir. Hedef konfigürasyonu ise diğer bir önemli faktör olup hedef kalınlığı arttıkça balistik direnç artmaktadır. Aynı kalınlığa sahip tek ve çift katmanlı hedefler birbirine yakın balistik davranış göstermektedir.

Anahtar Kelimeler: Zırh levhası, alüminyum, balistik çarpma, sonlu elemanlar yöntemi.

1. INTRODUCTION

Aluminum plates are extensively utilized in armor systems due to their high strength to weight ratio. Investigations into the protective performance of aluminum alloys were initiated in the early 1940s and the primary objective was to achieve improved protection against fragmentation by artillery shells. Aluminum alloys especially 5083 alloys are designated for specific armor applications which are strengthened by work hardening to increase their ballistic resistance to fragment penetration. These alloys are characterized by proper formability, weldability and structural strength. Armor made of 5083 alloy has been widely used for ballistic protection in many applications, the most notable of which is the M113 Personnel Carrier hull structure [1].

Elaldi et al. [2] studied the influence of impactor geometry on various targets. Based on this study, conical and ogival type penetrators exhibited more penetrative effect in comparison to impactors with larger contact surfaces such as flat-ended ones. Iqbal et al. [3] investigated the ballistic limits of targets with different configurations such as monolithic and multilayer targets. An ogive nose projectile was used in the impact tests and according to this study, each target exhibits different ballistic limits as the obliquity is changed in the targets. Singh et al. [4] used functionally graded plates as the targets in oblique low velocity impacts. Nishida et al. [5] studied the local damage of composites panels subjected to oblique projectile impacts. A parametric approach was carried out using simulations which were verified by experimental results. Forrestal et al. [6] investigated conical and ogival nose rigid rod projectiles that perforate 5083-H131 and 6061-T651aluminum armor plates. Børvik et al. [7] studied the ballistic resistance of 5083-H116 aluminum armor plates under rigid and conical nose rod impact. Gooch et al. [8] presented the ballistic limit data for 6061-T651 aluminum plates. Borvik et al. [9] studied the ballistic limit of 12 mm thick Weldox steel

*Sorumlu yazar (Corresponding Author)
e-mail:: sgurgen@ogu.edu.tr

plates for projectiles with various nose. They found that the ballistic limit is 185 and 300 m/s for blunt and conical projectiles respectively. Gupta et al. [10] investigated the perforation of aluminum plates under ballistic conditions. It was reported that ogive nose projectile is most efficient penetrator for 0.5 to 1.5 mm thickness aluminum plates while blunt projectiles are suggested for 2 to 3 mm thickness aluminum plates. Iqbal et al. [11] studies the influence of projectile nose angle on the ballistic limit of 12 mm thick Weldox steel plates. It was suggested that the ballistic limit of these plates linearly increases with the decrease in the projectile nose angle from 180º to 33.4º. Yoshizawa et al. [12] showed that the ballistic resistance of steel plates with the thickness of 7 to 38 mm decreases as the nose angle of projectile decreases. Jones et al. [13] investigated the perforation of aluminum alloys under low and moderate velocity impact conditions. They recommended empirical equations that are suitable for estimating the perforation energy of the plates. Forrestal et al. [14]–[16] used analytical modeling to calculate the penetration depth and perforation resistance of different materials. Paik et al. [17] investigated the characteristics of deformation and perforation on thin-walled structures under ballistic impact based on numerical simulations. They presented an empirical formula that relates impact energy absorbed up to perforation of the target plate with the impact velocity of projectile. Dey et al. [18] studied the ballistic resistance of double layered steel targets impacted by blunt and ogival nose projectiles. It was found that double layered plates offer a large gain in ballistic limit against blunt projectiles but the advantage disappears against ogival projectiles. Liu et al. [19] numerically investigated the perforation of Weldox steel and 5083-H116 aluminum alloy targets. It was suggested that the proposed material model is effective to predict the failure characteristics of the targets based on the experimental outputs.

Despite the several investigations into the ballistic resistance of metal plates in the literature, oblique impacts have not been studied extensively. The majority of ballistic studies focus on the worst case scenario with normal impact conditions where the angle between the projectile travel direction and the normal vector of target is zero. However, most of the real conditions has some degree of obliquity in the projectile impact on targets. Oblique impact on targets was only discussed in early review papers [20]–[23]. Beside the review papers, more recent investigations into the oblique impact on different targets can be found in [24]–[26]. In this paper, oblique impact of rigid ogive nose projectile on 5083-H116 aluminum alloy plates was numerically investigated. The numerical model was validated using experimental results of Børvik et al. [27] where the targets were subjected to rigid projectile perforation with the impact angle of 90º. In the present study, three parameters such as impact velocity, impact angle and target configuration were varied to observe their influence in the ballistic impacts. Based on the results, the oblique angle of impact acts an important role on the deformation mode of targets. The penetration of projectile dominates targets under low oblique angle impacts and the deformation changes from embedment to ricochet as oblique angle increases. Beside the oblique angle, the ballistic resistance of target is heavily dependent on impact velocity. As it is expected, targets are easily perforated as impact velocity increases even if oblique angle becomes larger. Target configuration is another factor on the protective performance which is increased using thicker plates. The ballistic response of monolithic and double layer targets for the same thickness is very close each other.

2. MATERIALS AND METHOD

2.1. Material Properties

In the study, 5083-H116 aluminum alloy was used as the target material. This alloy has the main alloying elements of 4.75 wt% magnesium, 0.84 wt% manganese and 0.18 wt% iron [7]. For the armor plates made of 5083-H116 aluminum alloys, the US Army Research Laboratory suggests some limit properties that the material should satisfy such as ultimate tensile strength of 283 MPa, yield strength of 200 MPa for 0.2% offset and percent elongation of 0.10 at tensile failure [28]. In order to obtain the mechanical properties of AA5083-H116 under ballistic conditions, comprehensive material tests were performed by Clausen et al. [29]. In their extended test program, approximately 100 specimens were subjected to mechanical testing in consideration of anisotropy, strain rate and temperature. Based on the results, Johnson Cook material model exhibits the most suitable behavior for this alloy. In early studies of Børvik et al. [30], [31], a modified Johnson Cook material model was suggested and this modified model showed good match with the experimental results. The modified model avoids the numerical difficulties in the strain rate part of the original model in case of very small strain rates such as static conditions. Therefore, modified Johnson Cook expresses the equivalent stress, damage parameter and strain at fracture as in the Eq. 1 to 3.

$$\sigma_{eq} = \left(A + B{\varepsilon_p}^n\right)\left(1+\dot{\varepsilon_p}\right)^C\left[1-\left(\frac{T-T_{room}}{T_{melt}-T_{room}}\right)^m\right] \quad (1)$$

$$D = \sum \frac{\Delta\varepsilon_p}{\varepsilon^f} \quad (2)$$

$$\varepsilon^f = \left[D_1 + D_2\, exp D_3\left(\frac{P}{\sigma_{eff}}\right)\right]\left(1+\dot{\varepsilon_p}\right)^{D_4}\left[1+D_5\left(\frac{T-T_{room}}{T_{melt}-T_{room}}\right)\right] \quad (3)$$

Table 1. Material properties and constants for AA5083-H116 [7], [29]

Elastic modulus (MPa)	Poisson's ratio	Density (kg/m^3)	Yield stress (MPa)	A (MPa)	B (MPa)	n	C	m	T_{melt} (K)	T_{room} (K)
70000	0.3	2700	230	124	456	0.252	0.008	0.859	893	293

In Eq. 1, $\dot{\varepsilon_p}$ is the plastic strain rate, T_{melt} and T_{room} are the melting and room temperatures respectively. In Eq. 3, P is the hydrostatic stress and σ_{eff} is the von Mises stress respectively. A, B, n, C and m are the material constants and D with sub-indices indicates the damage constants. D_1, D_2 and D_3 are associated with the impact stress triaxiality ratio (P/σ_{eff}). D_4 and D_5 are related to the strain rate and temperature respectively. There are five material parameters required to find the equivalent stress for the modified Johnson Cook model. The first three parameters; A, B, n describe the elasto-plastic deformation of the material, the fourth and fifth parameters; C and m define the strain rate and temperature influences.

The material parameters of AA5083-H116 were obtained from the previous studies by Børvik et al. [7], [29]. It was stated that material strength properties may exhibit minor deviations with respect to the plate thickness due to the manufacturing stage of the materials. Therefore, the values were selected for 20 mm thick plates which is used in this study. Table 1 gives the material properties and constants for the target plates.

2.2. Numerical Modeling and Validation

Numerical simulations were carried out using Ls-Dyna software. The target was modeled as a square plate with 600 mm length and 20 mm thickness as in the reference study. The hardened steel projectile with the mass of 0.197 kg was considered as a rigid body. Figure 1 shows the dimensions of the projectile used in this study. In the numerical modeling, axisymmetric conditions were applied to reduce time expense in the solution. 8-node brick elements with reduced integration were used to mesh the components. The target was fully clamped at the edge boundaries. Mesh density was increased in the impact zone using finer size elements and the size of the elements was gradually increased apart from the deformation point. At the center of the plate, mesh size was used as 0.1 mm and the largest mesh size of 0.5 mm was used at the corners as shown in Figure 2. The constitutive behavior was modeled using the modified Johnson Cook relation given in Eq. 1. Element erosion was enabled to prevent excessively distorted elements which could cause error termination by reducing the time step. Contact between the parts was established using a surface to surface algorithm and no gap condition was considered between the plates in double layer target. A friction coefficient of 0.5 was considered between the projectile and targets as suggested in an early work [25].

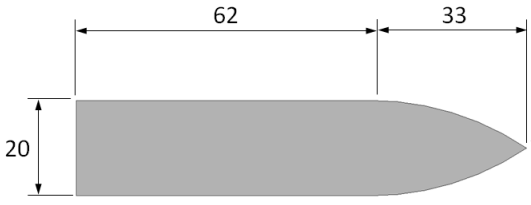

Figure 1. Dimensions of the ogive nose projectile

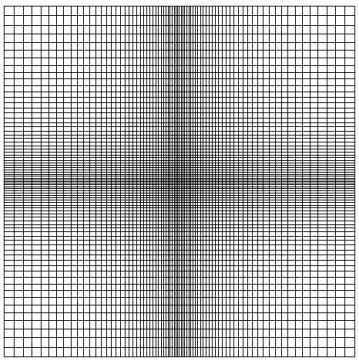

Figure 2. Non-uniform plate mesh

$$CI = 1 - \left[\frac{\sum {e_i}^2}{\sum {Vr_{exp}}^2}\right]^{1/2} \quad (4)$$

In the experimental validation of the numerical model, residual velocity of the projectile was compared with the experimental results of Børvik et al. [27]. The reference study used five different impact velocities in the range of 242.1–360.3 m/s. Figure 3 shows the comparison of the residual velocities in the experiments and simulations. Based on the experimental results, the ballistic limit velocity was obtained as 244 m/s. Figure 4 shows the target in experiment and simulation after the projectile impact with the velocity of 242.1 m/s. The deformed targets showed that the size of the holes are approximately identical with the diameter of the projectile which means the material exhibits ductile, hole-growth deformation as given in [27]. In order to assess the correlation degree of simulation based residual velocities with experimental residual velocities, a "Correlation Index" (CI) is defined in Eq. 4 as suggested by Raguraman et al. [32] where e_i represents the difference between the computed and experimental residual velocities while Vr_{exp} represents the residual velocity in experiments. It is obvious that CI approaches unity for perfect match conditions. In this study, CI is calculated as 0.913 which means the residual velocities in the simulations exhibit good agreement with the experiments and thus, the numerical model could be accepted to investigate the targets under ballistic impact.

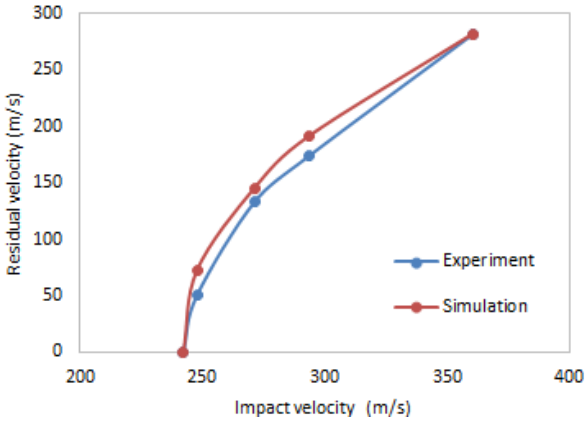

Figure 3. Residual velocities in experiments and simulations

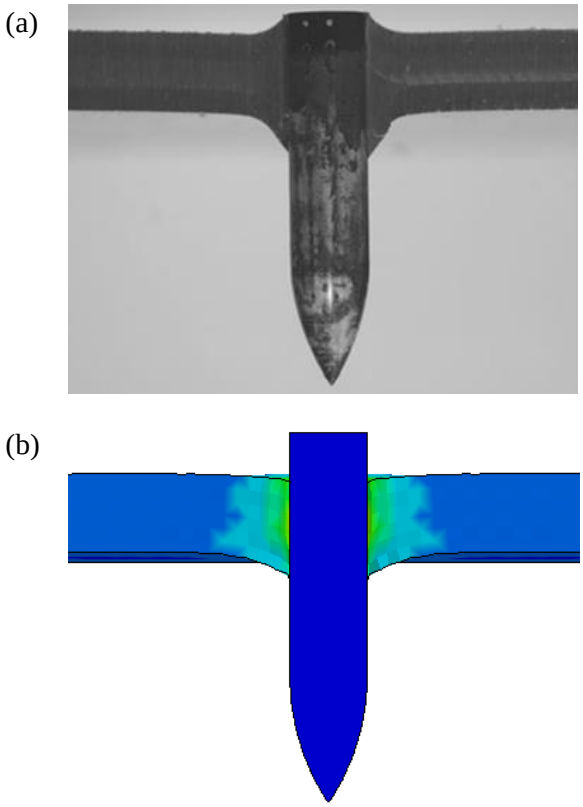

Figure 4. Target perforation after the projectile impact with the velocity of 242.1 m/s in the (a) experiment and (b) simulation

3. DESIGN OF THE OBLIQUE IMPACTS

In the present study, three variable parameters (target configuration, oblique angle and impact velocity) were applied with various levels. Target configuration was designed with monolithic and double-layer plates. Monolithic targets were used with 20 and 40 mm plates while double-layer target was assembled with two 20 mm thick plates. Oblique angle of the impacts was illustrated in Figure 5 and decided as 30º, 45º and 60º. The projectile impacted the targets with four different velocities such as 240, 360, 480 and 600 m/s. According to the full factorial design, simulations were set as given in Table 2.

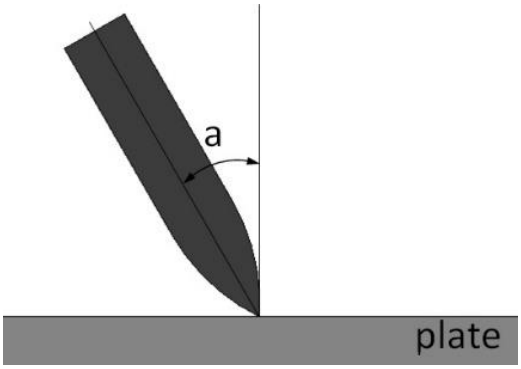

Figure 5. Oblique angle of the impact

Table 2. Design of the simulations

Level	Target configuration	Oblique angle	Impact velocity (m/s)
1	Monolithic-20	0º	240
2	Monolithic-40	30º	360
3	Double	45º	480
4	-	60º	600

4. RESULTS AND DISCUSSION

In the oblique impacts with the projectile velocity of 240 m/s, each target stops the projectile in different manners. The projectile ricochets off the target surface when the oblique angle is 60º whereas the projectile with the oblique angles of 30º and 45º embeds into the targets. Figure 6 and Figure 7 shows the embedded projectiles into the targets after 240 m/s velocity impacts with the oblique angle of 30º and 45º respectively. In fact, assessment of the deformation in the target is dependent on the different standards which were adopted by various institutes. According to the US Army, perforation is achieved even if the projectile is embedded in the target but light can pass through it. However, the US Navy defines perforation when the projectile fully emerges from the target [33]. Based on these various definitions, the deformation shown in Figure 6a is called a perforation according to the US Army criterion whereas a partial penetration according to the US Navy criterion where the projectile is stopped in the target. In this study, the US Navy criterion is considered in the evaluation of the deformations after the impacts. In this light, the targets introduces perforation as the impact velocity increases. However, for the oblique angle of 60º, each target avoids of perforation under the impact velocity of 360 m/s and the targets except for 20 mm thick monolithic plate stop the projectile under the impact velocity of 480 m/s. As depicted in Figure 8, as the oblique angle increases, the projectile path along the target increases and therefore, target could stop the projectile even if the impact velocity increases. It is possible to mention that targets hinder the perforation as the oblique angle increases and the failure mode in the target turns from projectile embedment to ricochet [34]. Furthermore, impact velocity dominates the failure in the target and therefore, the projectile could perforate each target even if the oblique angle is 60º when the impact velocity reaches 600 m/s.

Based on the results, ogive nose projectile penetrates the target mainly by ductile, hole-growth deformation pushing the material in front of the projectile aside as stated by Børvik et al. [9], [27] for normal impact conditions. Beside the material properties, projectile nose geometry is significant on the deformation type in the impacted targets. Generally, curved or sharp nose projectiles such as hemispherical, conical and ogive types cause hole-growth failure mode in thick targets due to the plunging of small sized nose tip with gradually enlarged diameter along the projectile length. However, ricochet

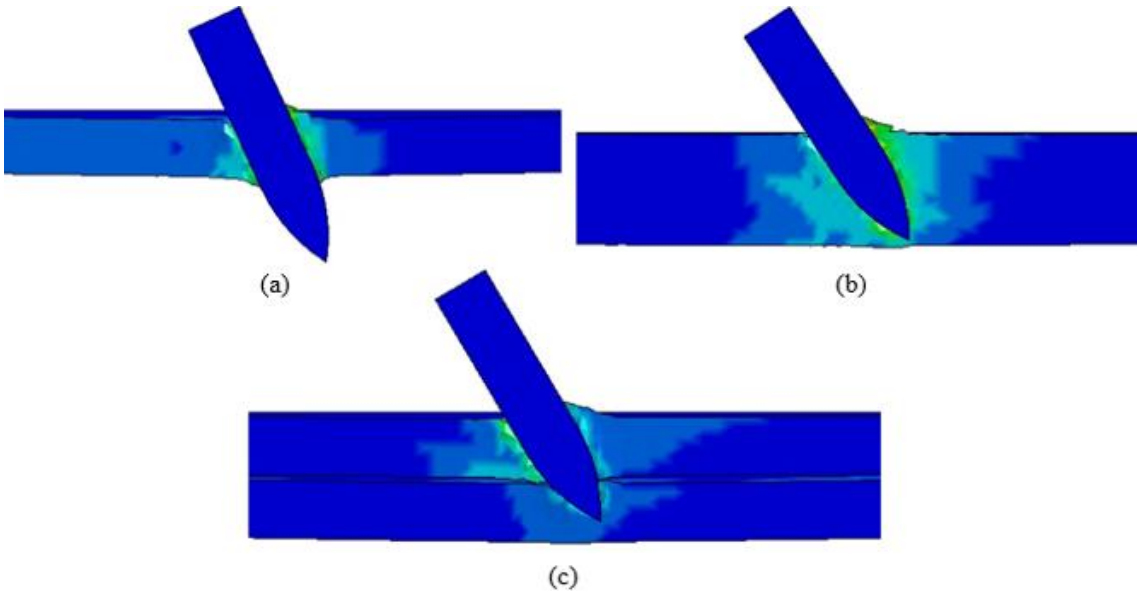

Figure 6. Embedded projectiles into (a) monolithic-20, (b) monolithic-40 and (c) double-layer target after 240 m/s velocity impacts with the oblique angle of 30º

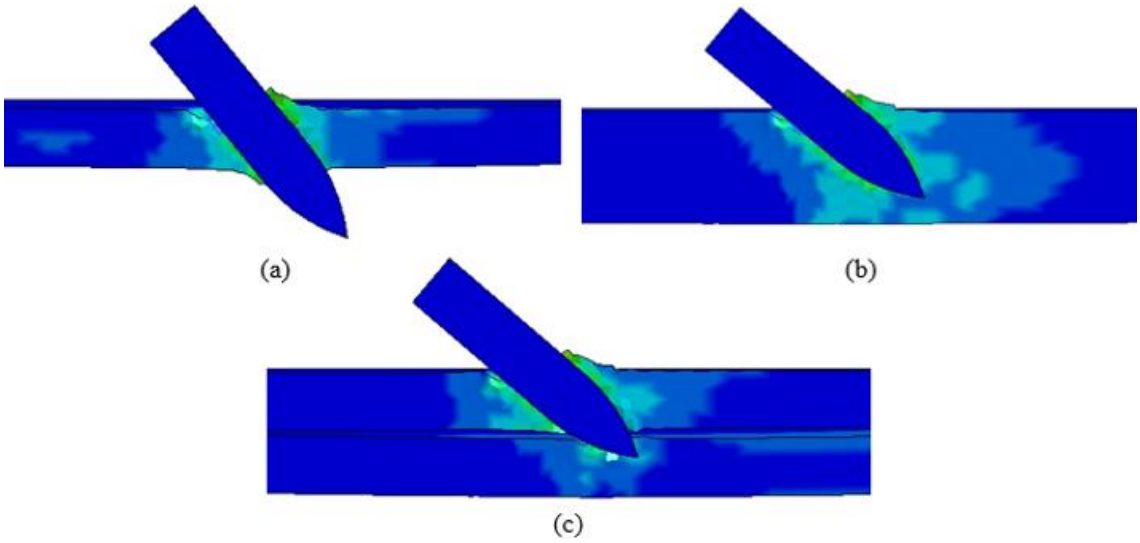

Figure 7. Embedded projectiles into (a) monolithic-20, (b) monolithic-40 and (c) double-layer target after 240 m/s velocity impacts with the oblique angle of 45º

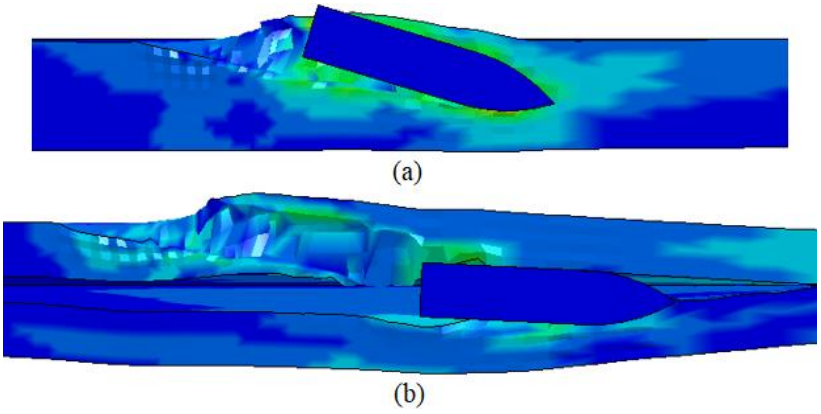

Figure 8. (a) 40 mm thick monolithic and (b) double layer targets after the impact velocity of 480 m/s with the oblique angle of 60º

of oblique angle since plunging of the projectile into the target becomes difficult due to high incidence angle. In thin targets, these projectiles are responsible for petalling causing radial cracking due to high circumferential strains and subsequent rotation of the deformed target material resulting in a number of petals. The targets even the 20 mm thick monolithic one do not exhibit petalling after the impacts and therefore, 20 mm thickness of AA5083-H116 plates could be evaluated as thick enough under the impacts by the used hardened steel ogive nose projectile.

Figure 9 shows the residual velocity versus impact velocity of the projectile for each target. It is obvious that residual velocity of the projectile increases by increasing the impact velocity due to the increased energy of the projectile. Considering the target configuration, 40 mm thick monolithic and double layer targets exhibit approximately identical responses in terms of residual velocity of the projectile. However, 20 mm thick monolithic target shows weaker protection performance and thereby allowing the projectile to emerge from the target with higher residual velocity. As expected, residual velocity decreases with the increase of areal density due to the increased energy absorption capacity in thicker targets. Same thickness targets such as 40 mm thick monolithic and double layer targets have identical areal densities and exhibit close protection performance. Almohandes et al. [35] stated that difference between the protection capacity of monolithic and multilayer targets with same thicknesses is very small especially under high velocity impacts. Furthermore, Flores-Johnson et al. [36] found that the difference in protective performance between monolithic and double layer aluminum plates is not significant for thicknesses less than 30 mm. However, reduction of penetration resistance in multilayer targets becomes notable when the number of plates is increased while keeping the total thickness constant. This weakening in multilayer configuration is due to the fact that bending stiffness reduces in the target.

Figure 10 shows the residual velocity versus oblique angle of the impacts for each impact velocity. It is obvious that residual velocity changes inversely with the oblique angle of impact. It is also noteworthy that residual velocity drastically decreases as the oblique angle changes from 45º to 60º. However, the difference between the oblique angle of 30º and 45º is not substantial. Based on the graphs, critical oblique angle at which the deformation changes from perforation to embedment or ricochet can be determined for each target. For example, the critical oblique angle is close to 60º for 40 mm thick monolithic and double layer targets under the impact velocity of 480 m/s while it can be predicted larger than 60º for 20 mm thick monolithic target.

Figure 11 shows the energy absorption capacity of the targets for each impact condition. Energy absorption capacity was calculated by the difference between the impact energy and the residual energy of the projectile. These terms were found from the kinetic energy formula using the impact and residual velocities. According to the results, target thickness plays an important role on the

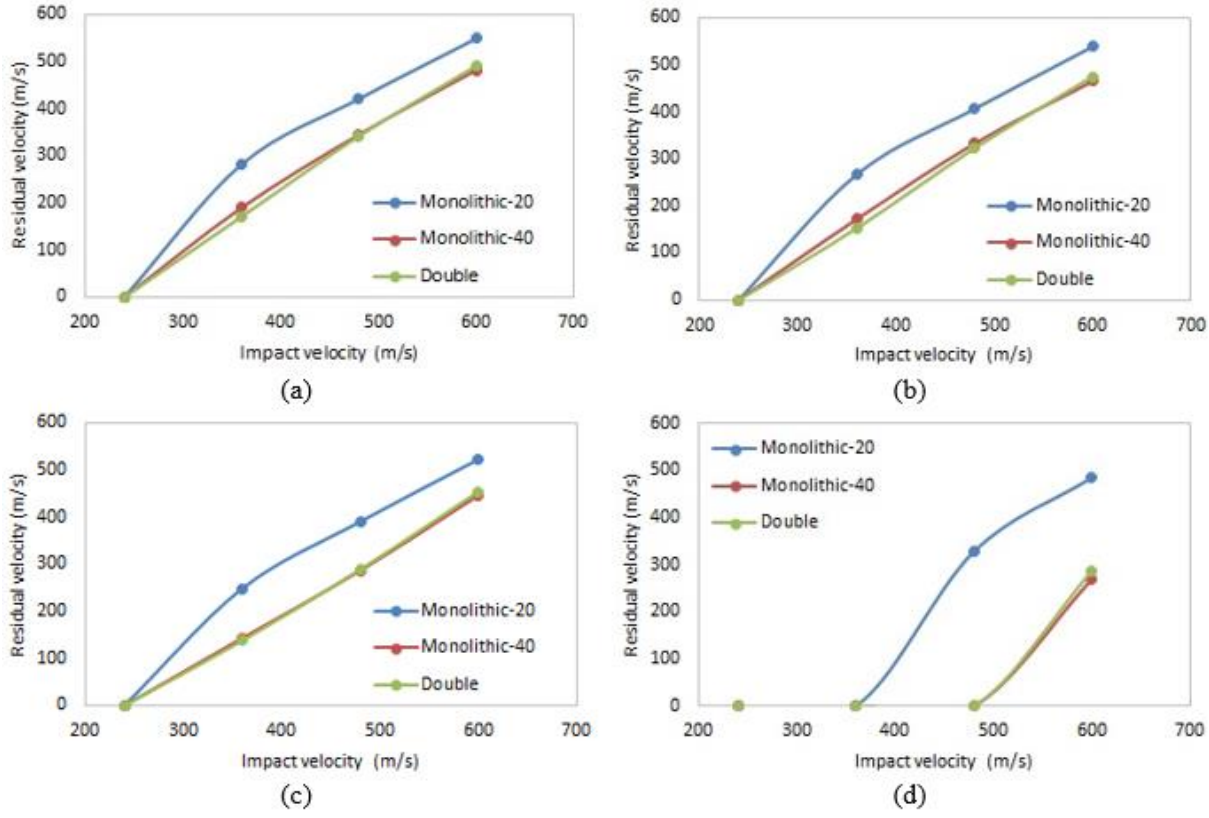

Figure 9. Residual velocity vs impact velocity for the oblique angle of (a) 0º, (b) 30º, (c) 45º and (d) 60º

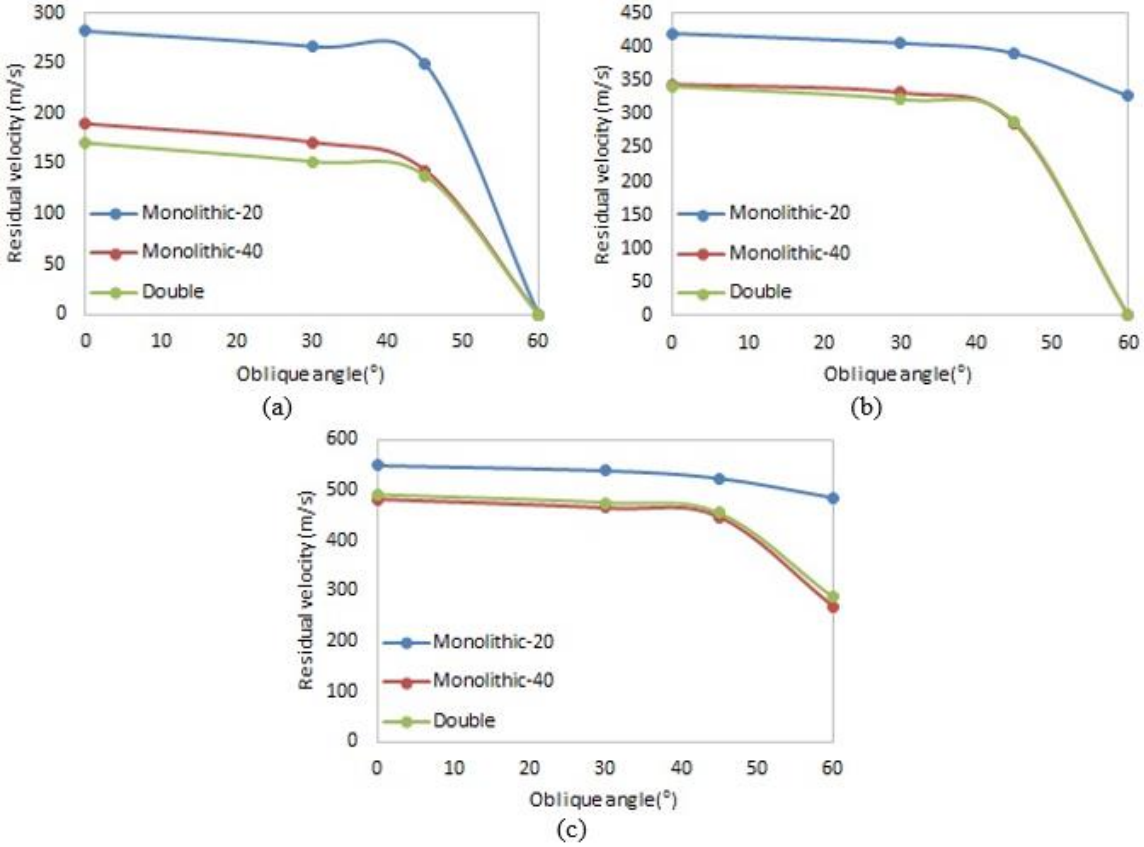

Figure 10. Residual velocity vs oblique angle for the impact velocity of (a) 360 m/s, (b) 480 m/s and (c) 600 m/s

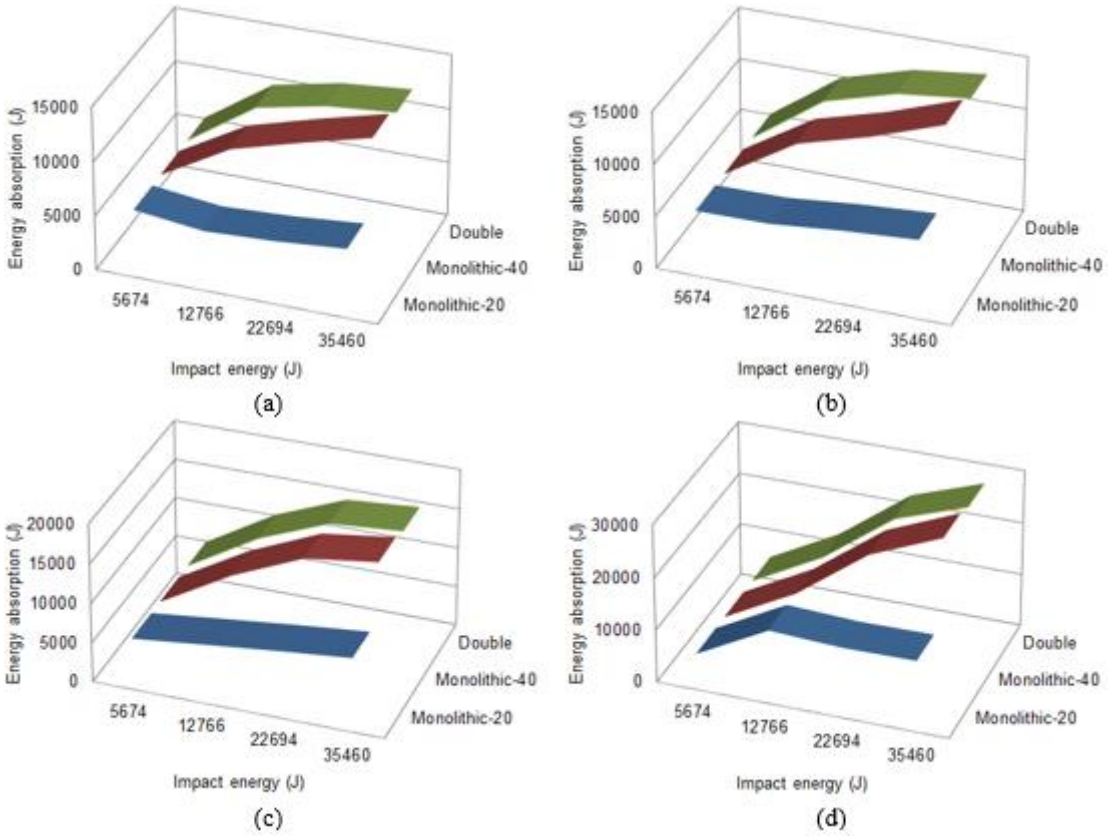

Figure 11. Energy absorption capacity of the targets for the oblique angle of (a) 30º, (b) 45º and (c) 60º

[37]. The plastic work done by the target increases with the thickness of target due to the increased areal density. Despite remaining identical areal densities, target configuration could change the protective performance of the targets. Considering the 40 mm thick monolithic and double layer targets, there is no significant difference in the energy absorption capacities. Hardly distinguishable from the high energy impacts, the monolithic target exhibits higher energy absorption capacity in comparison to the double layer target. This difference is pronounced as the impact energy increases and therefore, monolithic plates rather than a multilayer configuration are suggested for the protective applications. Regarding this point, deflection of the plates negatively influences the energy absorption capacity of the target as stated early investigations [35], [36]. Multilayer targets are assembled with a number of relatively thin plates and each plate exhibits lower bending resistance in comparison to a monolithic plate having the same thickness with the multilayer target. For this reason, multilayer targets have more deflection under impact which causes reduction in the energy absorption capacity.

5. CONCLUSIONS

In the present study, oblique impacts on AA5083-H116 plates were numerically investigated. The verification of the numerical model was performed using the experimental results of an early study [27]. The effects of three variable parameters such as impact velocity, impact angle and target configuration were investigated on the ballistic resistance of targets. Based on the results, the oblique angle of impact acts an important role on the deformation mode of targets. The penetration of projectile dominates targets under low oblique angle impacts and the deformation changes from embedment to ricochet as oblique angle increases. Beside the oblique angle, the ballistic resistance of target is heavily dependent on impact velocity. As it is expected, targets are easily perforated as impact velocity increases even if oblique angle becomes larger. Target configuration is another factor on the protective performance which is increased using thicker plates. Although the ballistic response of monolithic and double layer targets for the same thickness is very close each other, monolithic targets are suggested especially against high velocity impacts.

REFERENCES

[1] Laible R. C., "Ballistic materials and penetration mechanics", ***Elsevier***, New York, USA, (1980).

[2] Elaldi F., Baykan B., and Akto C., "Experimental Analysis for the Effect of Impactor Geometry on Carbon Reinforced Composite Materials", ***Polymers & Polymer Composites***, 25(9): 677–682, (2017).

[3] Iqbal M. A., Senthil K., Madhu V., and Gupta N. K., "Oblique impact on single, layered and spaced mild steel targets by 7.62 AP projectiles", ***Int. J. Impact Eng.***, 110: 26–38, (2017).

[4] Singh H., Hazarika B. C., and Dey S., "Low Velocity Impact Responses of Functionally Graded Plates", ***Procedia Eng.***, 173: 264–270, (2017).

[5] Nishida A., Ohta Y., Tsubota H., and Li Y., "A Study for Evaluating Local Damage to Reinforced Concrete Panels Subjected to Oblique Impact of Deformable Projectile", ***ASME Pressure Vessels and Piping Conference***, Hawaii, USA, 1–10, (2017).

[6] Forrestal M. J. and Warren T. L., "Perforation equations for conical and ogival nose rigid projectiles into aluminum target plates", ***Int. J. Impact Eng.***, 36(2): 220–225, (2009).

[7] Børvik T., Forrestal M. J., Hopperstad O. S., Warren T. L. and Langseth M., "Perforation of AA5083-H116 aluminium plates with conical-nose steel projectiles – Calculations", ***Int. J. Impact Eng.***, 36(3): 426–437, (2009).

[8] Gooch W., Burkins M. S. and Squillacioti R. J., "Ballistic testing of commercial aluminum alloys and alternative processing techniques to increase the availability of aluminum armor", ***23rd International Symposium on Ballistics***, Tarragona, Spain, 981–988, (2007).

[9] Børvik T., Langseth M., Hopperstad O. S., and Malo K., "Perforation of 12mm thick steel plates by 20mm diameter projectiles with flat, hemispherical and conical noses", ***Int. J. Impact Eng.***, 27(1): 19–35, (2002).

[10] Gupta N. K., Iqbal M. A., and Sekhon G. S., "Effect of projectile nose shape, impact velocity and target thickness on deformation behavior of aluminum plates", ***Int. J. Solids Struct.***, 44(10): 3411–3439, (2007).

[11] Iqbal M. A., Gupta G., Diwakar A., and Gupta N. K., "Effect of projectile nose shape on the ballistic resistance of ductile targets", ***Eur. J. Mech. – A Solids***, 29(4): 683–694, (2010).

[12] Yoshizawa H., Ohte S., Kashima Y., Chiba N., and Shida S., "Impact Strength of Steel Plates Struck by Projectiles : Effect of Mechanical Properties on Critical Fracture Energy", ***Bull. JSME***, 27(226): 639–644, (1984).

[13] Jones N. and Paik J. K., "Impact perforation of aluminium alloy plates", ***Int. J. Impact Eng.***, 48: 46–53, (2012).

[14] Piekutowski A. J., Forrestal M. J., Poormon K. L., and Warren T. L., "Perforation of aluminum plates with ogive-nose steel rods at normal and oblique impacts", ***Int. J. Impact Eng.***, 18(7–8): 877–887, (1996).

[15] Forrestal M. J., Luk V. K., and Brar N. S., "Perforation of aluminum armor plates with conical-nose projectiles", ***Mech. Mater.***, 10(1–2): 97–105, (1990).

[16] Rosenberg Z. and Forrestal M. J., "Perforation of Aluminum Plates with Conical-Nosed Rods—Additional Data and Discussion", ***J. Appl. Mech.***, 55(1): 236-244, (1988).

[17] Paik J. K. and Won S. H., "On deformation and perforation of ship structures under ballistic impacts", ***Ships Offshore Struct.***, 2(3): 217–226, (2007).

[18] Dey S., Børvik T., Teng X., Wierzbicki T., and Hopperstad O. S., "On the ballistic resistance of double-layered steel plates: An experimental and numerical investigation", ***Int. J. Solids Struct.***, 44(20): 6701–6723, (2007).

[19] Liu Z. S., Swaddiwudhipong S., and Islam M. J., "Perforation of steel and aluminum targets using a

modified Johnson–Cook material model", ***Nucl. Eng. Des.***, 250: 108–115, (2012).

[20] Backman M. E. and Goldsmith W., "The mechanics of penetration of projectiles into targets", ***Int. J. Eng. Sci.***, 16(1): 1–99, (1978).

[21] Johnson W., Sengupta A. K., and Ghosh S. K., "High velocity oblique impact and ricochet mainly of long rod projectiles: An overview", ***Int. J. Mech. Sci***., 24(7): 425–436, (1982).

[22] Corbett G. G., Reid S. R., and Johnson W., "Impact loading of plates and shells by free-flying projectiles: A review", ***Int. J. Impact Eng***., 18(2): 141–230, (1996).

[23] Goldsmith W., "Non-ideal projectile impact on targets", ***Int. J. Impact Eng***., 22(2–3): 95–395, (1999).

[24] Iqbal M. A., Gupta G., and Gupta N. K., "3D numerical simulations of ductile targets subjected to oblique impact by sharp nosed projectiles", ***Int. J. Solids Struct.***, 47(2): 224–237, (2010).

[25] Iqbal M. A., Chakrabarti A., Beniwal S., and Gupta N. K., "3D numerical simulations of sharp nosed projectile impact on ductile targets," ***Int. J. Impact Eng***., 37(2): 185–195, (2010).

[26] Zhou D. W. and Stronge W. J., "Ballistic limit for oblique impact of thin sandwich panels and spaced plates", ***Int. J. Impact Eng***., 35(11): 1339–1354, (2008).

[27] Børvik T., Forrestal M. J., and Warren T. L., "Perforation of 5083-H116 Aluminum Armor Plates with Ogive-Nose Rods and 7.62 mm APM2 Bullets", ***Exp. Mech.***, 50(7): 969–978, (2010).

[28] US Army Research Laboratory, "Armor plate, aluminum alloy, weldability 5083, 5456, and 5059", ***Military Specifications,*** MIL-DTL-46027 K (2007).

[29] Clausen A. H., Børvik T., Hopperstad O. S., and Benallal A., "Flow and fracture characteristics of aluminium alloy AA5083–H116 as function of strain rate, temperature and triaxiality", ***Mater. Sci. Eng. A***, 364(1–2): 260–272, (2004).

[30] Børvik T., Hopperstad O. S., Berstad T., and Langseth M., "Numerical simulation of plugging failure in ballistic penetration", ***Int. J. Solids Struct.***, 38(34–35): 6241–6264, (2001).

[31] Børvik T., Hopperstad O. S., Berstad T., and Langseth M., "A computational model of viscoplasticity and ductile damage for impact and penetration", ***Eur. J. Mech. – A Solids***, 20(5): 685–712, (2001).

[32] Raguraman M., Deb A., and Gupta N. K., "CAE-based prediction of projectile residual velocity for impact on single and multi-layered metallic armour plates", ***Latin American Journal of Solids and Structures***, 6: 247–263, (2009).

[33] Rosenberg Z. and Dekel E., "Terminal Ballistics", ***Springer,*** Berlin, Germany, (2014).

[34] Zukas J. A., "Impact dynamics", ***Wiley,*** New York, USA, (1982).

[35] Almohandes A. A., Abdel-Kader M. S., and Eleiche A. M., "Experimental investigation of the ballistic resistance of steel-fiberglass reinforced polyester laminated plates", ***Compos. Part B Eng.***, 27(5): 447–458, (1996).

[36] Flores-Johnson E. A., Saleh M., and Edwards L., "Ballistic performance of multi-layered metallic plates impacted by a 7.62-mm APM2 projectile", ***Int. J. Impact Eng***., 38(12): 1022–1032, (2011).

[37] Corran R. S. J., Shadbolt P. J., and Ruiz C., "Impact loading of plates – An experimental investigation", ***Int. J. Impact Eng.***, 1(1): 3–22, (1983).